Krüppel-like factor 17 upregulates uterine corin expression and promotes spiral artery remodeling in pregnancy

Can Wang[a], Zhiting Wang[a], Meiling He[a], Tiantian Zhou[a], Yayan Niu[a,b], Shengxuan Sun[c], Hui Li[a], Ce Zhang[a], Shengnan Zhang[a], Meng Liu[a], Ying Xu[d], Ningzheng Dong[a,b,1], and Qingyu Wu[a,e,1]

[a]Cyrus Tang Hematology Center, Ministry of Education Engineering Center of Hematological Diseases, Collaborative Innovation Center of Hematology, State Key Laboratory of Radiation Medicine and Prevention, Soochow University, 215123 Suzhou, China; [b]Ministry of Health Key Laboratory of Thrombosis and Hemostasis, Jiangsu Institute of Hematology, The First Affiliated Hospital of Soochow University, 215006 Suzhou, China; [c]Department of Orthopedics, The Second Affiliated Hospital of Soochow University, 215004 Suzhou, China; [d]Cambridge-Soochow University Genomic Resource Center, Soochow University, 215123 Suzhou, China; and [e]Cardiovascular & Metabolic Sciences, Lerner Research Institute, Cleveland Clinic, Cleveland, OH 44195

Edited by R. Michael Roberts, University of Missouri, Columbia, MO, and approved June 25, 2020 (received for review February 29, 2020)

Spiral artery remodeling is an important physiological process in the pregnant uterus which increases blood flow to the fetus. Impaired spiral artery remodeling contributes to preeclampsia, a major disease in pregnancy. Corin, a transmembrane serine protease, is up-regulated in the pregnant uterus to promote spiral artery remodeling. To date, the mechanism underlying uterine corin up-regulation remains unknown. Here we show that Krüppel-like factor (KLF) 17 is a key transcription factor for uterine corin expression in pregnancy. In cultured human uterine endometrial cells, KLF17 binds to the *CORIN* promoter and enhances the promoter activity. Disruption of the *KLF17* gene in the endometrial cells abolishes *CORIN* expression. In mice, *Klf17* is up-regulated in the pregnant uterus. *Klf17* deficiency prevents uterine *Corin* expression in pregnancy. Moreover, *Klf17*-deficient mice have poorly remodeled uterine spiral arteries and develop gestational hypertension and proteinuria. Together, our results reveal an important function of KLF17 in regulating *Corin* expression and uterine physiology in pregnancy.

corin | KLF17 | pregnancy

In pregnancy, uterine spiral arteries undergo a remodeling process during which smooth muscle cells in the vessel wall and the lumen-lining endothelial cells are replaced by placenta-derived trophoblasts (1). The remodeled spiral arteries are highly dilated, thereby lowering maternal vascular resistance and increasing blood supply to the fetus. Preeclampsia is a disease afflicting ∼5 to 8% of pregnant women and causing maternal and fetal deaths (2). Impaired spiral artery remodeling is a major factor in the pathogenesis of preeclampsia (2–4). To date, the molecular mechanisms underlying spiral artery remodeling are not fully understood.

Atrial natriuretic peptide (ANP) is a cardiac hormone that regulates salt-water balance and blood pressure (5). It is synthesized as a precursor, i.e., pro-ANP, which is converted to mature ANP by corin, a transmembrane serine protease highly expressed in the heart (6, 7). In addition to the heart, corin and ANP are expressed in noncardiac tissues, such as kidneys (8–10), hair follicles (11, 12), and developing bones (13, 14). Recently, we and others have shown that corin is up-regulated in the pregnant uterus, where corin and ANP promote trophoblast invasion and spiral artery remodeling (15, 16). In pregnant mice, corin and ANP deficiency impairs spiral artery remodeling, causing gestational hypertension and proteinuria, a preeclampsia-like phenotype (15, 17, 18). In humans, reduced corin messenger RNA (mRNA) and protein levels and deleterious *CORIN* variants have been reported in preeclamptic women (15, 19, 20). These data indicate that uterine corin up-regulation is a part of the physiological response in normal pregnancy. It remains unknown, however, how corin expression is regulated in the pregnant uterus.

In the heart, natriuretic peptide expression is controlled by GATA-4, a zinc finger transcription factor (21, 22). A similar GATA-4–dependent mechanism is critical for cardiac corin expression. We have shown that human and mouse corin gene promoters contain a conserved sequence that is essential for GATA-4 binding and corin expression in cardiomyocytes (23). GATA-4 is primarily a cardiac transcription factor but not expressed in the uterus (24). It is likely that the transcriptional mechanism controlling corin expression in the uterus differs from that in the heart.

To test this hypothesis, we analyzed *CORIN* promoter activities in endometrial and cardiac cells. We also examined corin and transcription factor expression in decidualized human endometrial cells and mouse pregnant uteruses. We identified Krüppel-like factor 17 (KLF17) as a key transcription factor for uterine corin expression. In mice, *Klf17* deficiency prevented *Corin* expression in the pregnant uterus. *Klf17*-deficient mice developed pregnancy-induced hypertension and proteinuria. These findings indicate an important role of KLF17 in *Corin* expression and uterine physiology in pregnancy.

Results

Human *CORIN* Promoter Activity in Uterine and Cardiac Cells. Previously, we identified a conserved GATA-binding sequence in the human *CORIN* promoter required for corin expression in

Significance

In pregnancy, blood vessels in the uterus increase in size, providing more blood supply and nutrients to the growing fetus. Corin is an enzyme that boosts this process. In this study, we sought to understand how uterine corin production is controlled. In experiments with human uterine cells and pregnant mice, we identified a protein, called Krüppel-like factor 17 (KLF17), which turns on the corin gene in the pregnant uterus. In genetically modified mice, Klf17 deficiency prevents uterine corin production, decreases uterine vessel size, and causes high blood pressure in pregnancy. These results show that KLF17 is a gene-controlling protein important for uterus function in pregnancy.

Author contributions: C.W., Z.W., N.D., and Q.W. designed research; C.W., Z.W., M.H., T.Z., Y.N., S.S., H.L., C.Z., S.Z., and M.L. performed research; Y.X. contributed new reagents/analytic tools; C.W., Z.W., M.H., T.Z., Y.N., S.S., H.L., M.L., Y.X., N.D., and Q.W. analyzed data; and C.W., N.D., and Q.W. wrote the paper.

The authors declare no competing interest.

This article is a PNAS Direct Submission.

[1]To whom correspondence may be addressed. Email: ningzhengdong@suda.edu.cn or wuq@ccf.org.

This article contains supporting information online at https://www.pnas.org/lookup/suppl/doi:10.1073/pnas.2003913117/-/DCSupplemental.

First published July 27, 2020.

cardiomyocytes (23). In this study, we analyzed a 405-bp *CORIN* promoter fragment containing the GATA-binding sequence (Fig. 1*A*). In a luciferase assay, the promoter activity was detected in human uterine endometrial AN3-CA cells and murine HL-1 cardiomyocytes, in which endogenous corin expression was reported (25, 26) (Fig. 1 *B* and *C*). Within this promoter fragment, an E-box–binding site and two KLF-binding sites were located up-stream of the GATA-binding site (Fig. 1*A* and *SI Appendix*, Fig. S1). Deletion of the E-box–binding site had little effect on the *CORIN* promotor activity in AN3-CA and HL-1 cells (Fig. 1 *A*–*C*). Further deletion of the two KLF-binding sites abolished the promoter activity in AN3-CA, but not HL-1, cells (Fig. 1 *A*–*C*), suggesting a possible role of the KLF-binding sites in corin expression in uterine endometrial cells.

To verify our results, we mutated the KLF-binding sites, individually or together (Fig. 1*D*). In the luciferase assay, the promoter fragment with mutations in individual KLF-binding sites had reduced activities in AN3-CA cells (Fig. 1*E*). When both of the KLF-binding sites were mutated, the promoter activity was abolished in AN3-CA, but not HL-1, cells (Fig. 1 *E* and *F*). Conversely, mutations in the GATA-binding site abolished the promoter activity in HL-1, but not AN3-CA, cells (Fig. 1 *G*–*I*). These results indicate that corin expression in uterine endometrial cells is controlled by a transcriptional mechanism involving KLF, but not GATA, transcription factor(s).

Uterine Corin and KLF Expression in Progesterone-Treated and Pregnant Mice. The KLF family has 17 members (27). To identify KLF member(s) responsible for corin expression in the pregnant uterus, we treated ovariectomized C57BL/6 mice with estrogen or progesterone (*SI Appendix*, Fig. S2*A*). By qRT-PCR, we found increased uterine *Corin* mRNA levels in progesterone-treated, but not estrogen-treated, mice compared with that in vehicle-treated mice (Fig. 2*A*). We next analyzed the uterine expression of all 17 *Klf* genes by qRT-PCR in ovariectomized mice treated with progesterone. We found increased uterine mRNA levels of *Corin*, *Klf2*, *Klf9*, *Klf15*, and *Klf17*, but not the of remaining *Klf* genes (Fig. 2*B* and *SI Appendix*, Fig. S2*B*). We confirmed these results by qRT-PCR analysis of uterus tissues from pregnant C57BL/6 mice at different gestational (G) days (Fig. 2*C*). These results indicate that Klf2, Klf9, Klf15, and Klf17 are possible candidates responsible for corin up-regulation in the pregnant uterus.

Effects of KLF Expression on *CORIN* Promoter Activity in Uterine Cells. To examine the function of the KLF candidates, we cotransfected AN3-CA cells with *CORIN* promoter constructs and plasmids expressing human KLF2, KLF9, KLF15, and KLF17 proteins. Increased promoter activities were found when plasmids expressing KLF2 and KLF17, but not KLF9 and KLF15, were cotransfected with a promoter construct with the KLF-binding sites (Fig. 3 *A* and *B*). By Western blotting, we confirmed recombinant KLF expression in the transfected cells (Fig. 3*C*). In these experiments, the promoter activities were not increased if the cotransfection was done using the *CORIN* promoter constructs with the KLF-binding sites deleted (Fig. 3*D*) or mutated (Fig. 3*E*). Unlike in AN3-CA cells, recombinant KLF2 and KLF17 expression in HL-1 cardiomyocytes did not increase the promoter activity when the *CORIN* constructs with or

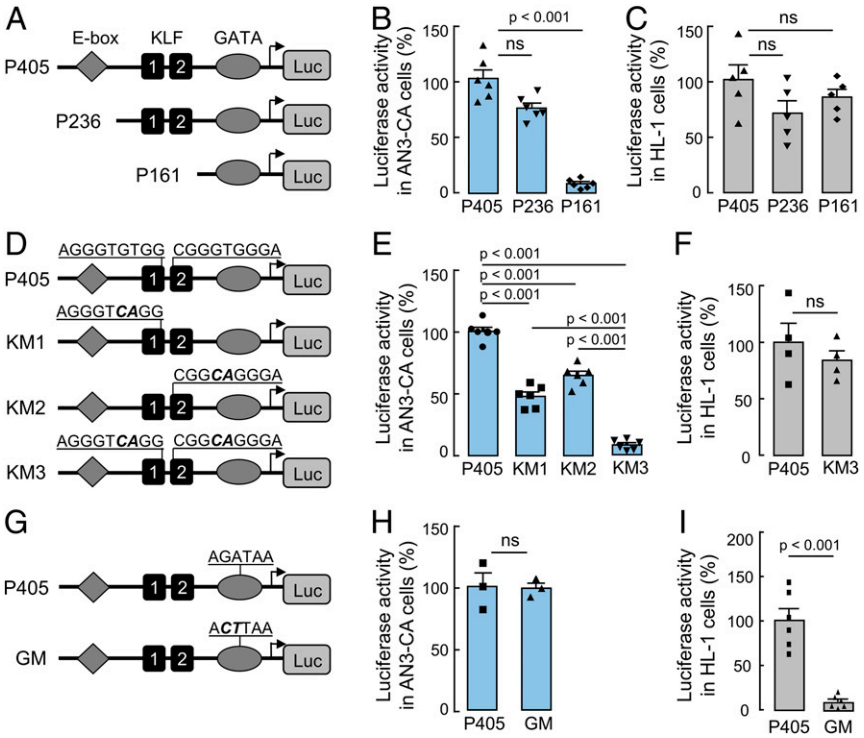

Fig. 1. *CORIN* promoter activities in uterine endometrial cells and cardiomyocytes. (*A*) Illustration of a luciferase construct with a 405-bp *CORIN* promoter fragment with an E-box–binding site, two KLF-binding sites, and a GATA-binding site (P405) and two constructs with 236- and 161-bp, respectively, truncated *CORIN* promoter fragments (P236 and P161). (*B* and *C*) Luciferase activities in endometrial AN3-CA (*B*) and HL-1 (*C*) cells transfected with the *CORIN* promoter constructs. The pGL3 construct was used as a background control. (*D*) Illustration of *CORIN* promoter constructs with mutations (boldface italic letters) in one (KM1 and KM2) or both (KM3) of the KLF-binding sites. (*E* and *F*) Luciferase activities in AN3-CA (*E*) and HL-1 (*F*) cells transfected with the *CORIN* promoter constructs. (*G*) Illustration of *CORIN* promoter construct with mutations (boldface italic letters) in the GATA-binding site (GM). (*H* and *I*) Luciferase activities in AN3-CA (*H*) and HL-1 (*I*) cells transfected with the *CORIN* promoter constructs. $n = 3$ to 6 per group. Data are presented as mean ± SEM; *P* values were analyzed by two-tailed Student's *t* test. ns, not significant.

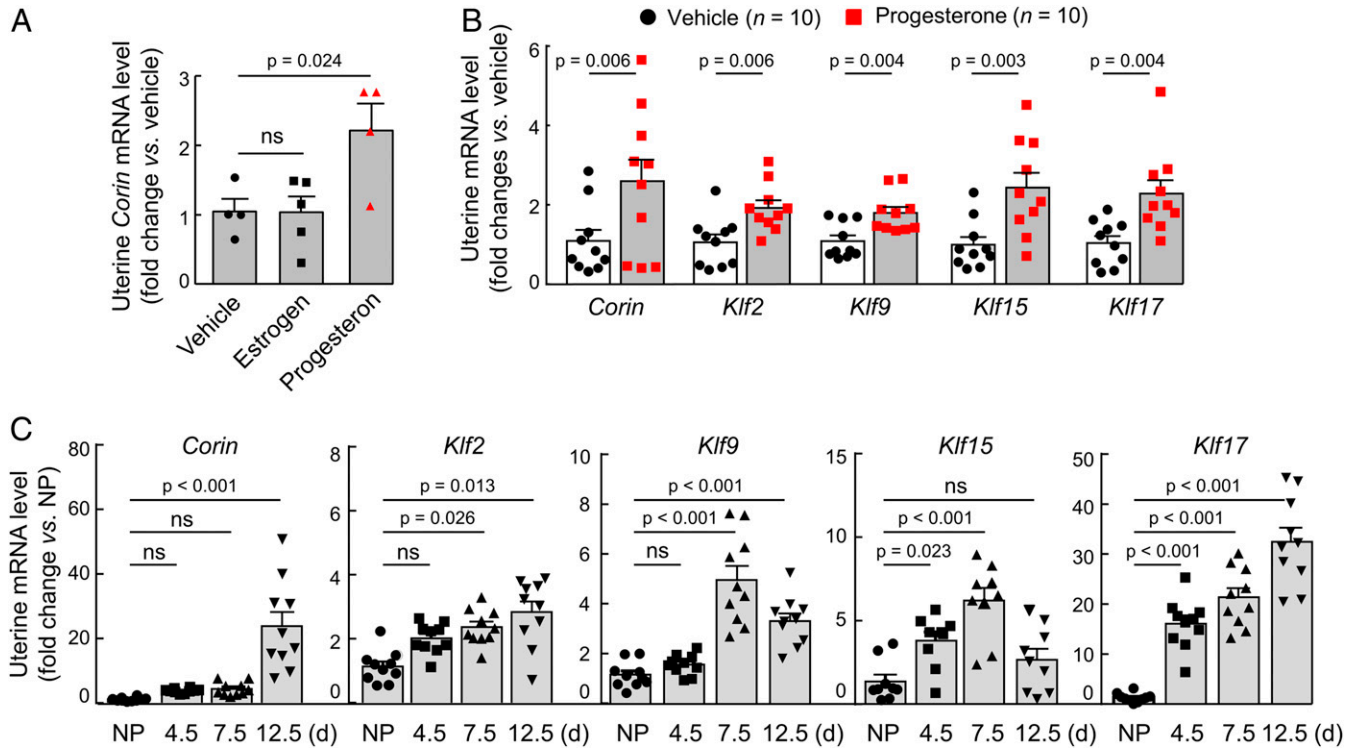

Fig. 2. *Corin* and *Klf* expression in mouse uteruses. (*A*) *Corin* mRNA levels in uteruses from ovariectomized mice treated with vehicle, estrogen, or progesterone. (*B*) *Corin*, *Klf2*, *Klf9*, *Klf15*, and *Klf17* mRNA levels in uteruses from ovariectomized mice treated with vehicle or progesterone. (*C*) *Corin*, *Klf2*, *Klf9*, *Klf15*, and *Klf17* mRNA levels in uteruses from nonpregnant (NP) and pregnant C57BL/6 mice at 4.5, 7.5, and 12.5 gestational days. $n = 4$ to 5 per group in *A*; $n = 10$ per group in *B*; $n = 9$ to 10 per group in *C*. Data are presented as mean ± SEM; *P* values were analyzed by ANOVA (*A* and *C*) or two-tailed Student's *t* test (*B*). ns, not significant.

without the KLF-binding sites were used (*SI Appendix*, Fig. S3 *A–D*). These results indicate that KLF2 and/or KLF17 are likely responsible for corin up-regulation in the pregnant uterus.

Increased Corin and KLF17 Expression in Decidualized Human Endometrial Stromal Cells. Human endometrial stromal cells (HESCs) are commonly used to induce decidualization in culture to mimic endometrial cells in the pregnant uterus (28). We cultured HESCs with the decidualization medium and detected increased *PRL* (encoding prolactin, a decidualization marker) and *CORIN* mRNA levels by qRT-PCR (Fig. 4*A*), consistent with corin up-regulation in the pregnant uterus (15). By Western blotting, increased KLF17 levels were found in the decidualized HESCs (Fig. 4*B*). In contrast, KLF2 levels were unchanged in similarly treated HESCs (Fig. 4*C*). We confirmed these results by immunohistochemistry (Fig. 4*D*) and coimmunofluorescent staining (Fig. 4*E*), which showed increased cytoplasmic and membrane staining of corin and nuclear staining of KLF17 in the decidualized, but not control, HESCs. Consistent with the Western blotting results, immunohistochemistry showed similar levels of nuclear KLF2 staining in the HESCs before and after decidualization (*SI Appendix*, Fig. S4).

Chromatin Immunoprecipitation Analysis. To examine if KLF17 binds directly to the *CORIN* promoter, we performed chromatin immunoprecipitation (ChIP) analysis in HESCs before and after decidualization. Positive PCR fragments were found when ChIP was done with an anti-KLF17 antibody in the decidualized, but not the control, HESCs (Fig. 5 *A* and *B*). In contrast, no PCR fragments were detected when control IgG or an anti-KLF2 or anti-KLF9 antibody was used (Fig. 5*B*). In positive controls, PCR fragments were detected when ChIP was done with an anti-histone 3 antibody in the HESCs before and after decidualization (Fig. 5*B*). The results were confirmed in additional qPCR analysis (*SI Appendix*, Fig. S5*A*), indicating that KLF17, but not KLF2, binds directly to the *CORIN* promoter in the decidualized HESCs.

Corin Expression in *KLF17*-Knockout HESCs. To determine KLF17 function in up-regulating corin expression in uterine endometrial cells, we disrupted the *KLF17* gene in HESCs using CRISPR/Cas9 (Fig. 5*C*). In Western blotting, no KLF17 protein was detected in *KLF17*-KO HESCs before or after decidualization (Fig. 5*D*). In qRT-PCR, highly increased *CORIN* mRNA levels were found in the decidualized HESCs compared with that in the control cells (Fig. 5*E*). Such up-regulation, however, was not found in *KLF17*-knockout (KO) HESCs (Fig. 5*E*). We confirmed these results in a separate line of *KLF17*-KO HESCs, in which the *KLF17* gene was disrupted at a different site in exon 1 (*SI Appendix*, Fig. S5 *B–D*). These data indicate a critical role of KLF17 in *CORIN* up-regulation in the decidualized human uterine endometrial cells.

Generation of *Klf17*$^{-/-}$ Mice. To understand the functional importance of Klf17 in vivo, we used mouse embryonic stem cells with a disrupted *Klf17* allele to generate *Klf17*$^{-/-}$ mice (*SI Appendix*, Fig. S6 *A* and *B*). *Klf17*$^{-/-}$ mice were viable without noticeable physical abnormalities. In necropsies and histological examinations, no apparent defects were found in major organs, including the testis where *Klf17* expression was reported (29). In RT-PCR, uterine *Klf17* and *Corin* up-regulation was detected in pregnant wild-type (WT), but not *Klf17*$^{-/-}$, mice (Fig. 6*A*). Consistently, qRT-PCR showed markedly decreased uterine *Corin* mRNA levels in pregnant *Klf17*$^{-/-}$ mice compared to those in pregnant WT mice (Fig. 6*B*). The results were confirmed by

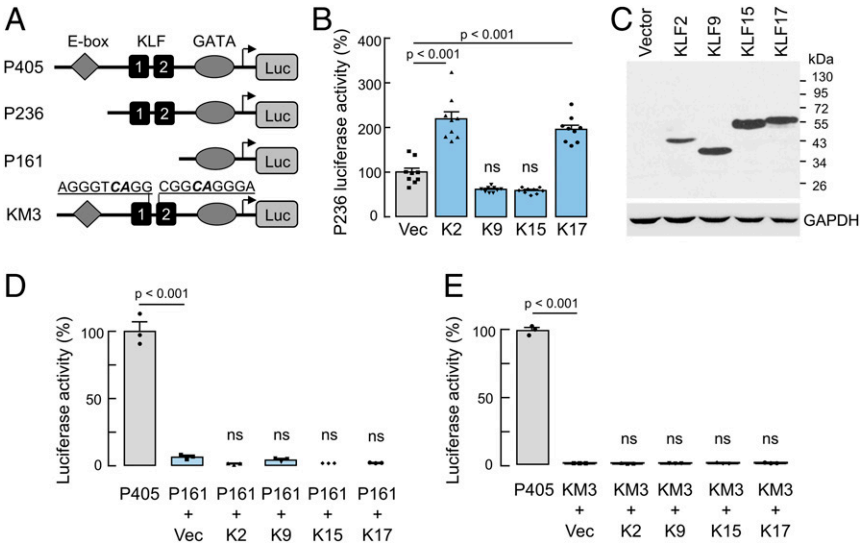

Fig. 3. Effects of recombinant KLF protein expression on *CORIN* promoter activities in uterine endometrial AN3-CA cells. (*A*) Illustration of *CORIN* promoter constructs used. (*B*) Luciferase activities in AN3-CA cells cotransfected with the P236 *CORIN* promoter construct and a control vector (Vec) or plasmids expressing human KLF2 (K2), KLF9 (K9), KLF15 (K15), or KLF17 (K17). $n = 8$ per group. Data are presented as mean ± SEM; *P* values were analyzed by ANOVA. ns, not significant. (*C*) Western blotting of recombinant KLF proteins in the transfected cells using an anti-FLAG antibody. (*D* and *E*) Luciferase activities in AN3-CA cells transfected with the P405 *CORIN* promoter construct (positive control) or cotransfected with the P161 (*D*) or KM3 (*E*) *CORIN* promoter construct and a control vector (Vec) or plasmids expressing human KLF2 (K2), KLF9 (K9), KLF15 (K15), or KLF17 (K17). $n = 3$ per group. Data are presented as mean ± SEM; *P* values (vs. P405) and ns (not significant) (vs. vector-cotransfected group) were analyzed by ANOVA.

Western blotting of Klf17 and Corin proteins in uterus samples from WT and $Klf17^{-/-}$ mice (*SI Appendix*, Fig. S7 *A* and *B*). In contrast, cardiac *Corin* mRNA levels were similar in nonpregnant and pregnant WT and $Klf17^{-/-}$ mice in RT-PCR and qRT-PCR analyses (*SI Appendix*, Fig. S7 *C* and *D*).

Fertility of $Klf17^{-/-}$ Male and Female Mice. We mated $Klf17^{+/-}$ mice and found the expected Mendelian ratio of $Klf17^{+/+}$, $Klf17^{+/-}$, and $Klf17^{-/-}$ offspring (Fig. 6*C*), indicating that there was no apparent embryonic loss in pregnant $Klf17^{+/-}$ mice. Mating $Klf17^{-/-}$ male and female mice, however, produced fewer pups per litter compared to those from $Klf17^{+/+}$ male and female mating (4.1 ± 0.3 [$n = 52$] vs. 7.1 ± 0.4 [$n = 22$]; $P < 0.01$) (Fig. 6*D*), indicating fetal demise in pregnant $Klf17^{-/-}$ mice. We next examined embryos in pregnant $Klf17^{+/+}$ and $Klf17^{-/-}$ mice that were mated with males of the same genotype. At G12.5 d, total embryos per mouse in $Klf17^{+/+}$ and $Klf17^{-/-}$ mice were similar (7.2 ± 0.5 [$n = 11$] vs. 7.6 ± 0.7 [$n = 17$]; $P = 0.64$) (Fig. 6*E*), suggesting similar fertilization and embryo implantation between $Klf17^{+/+}$ and $Klf17^{-/-}$ mice. In $Klf17^{-/-}$ mice, however, some of the embryos (29/90, 32.2%) were small and abnormal, whereas the other embryos (61/90, 67.7%) were indistinguishable in size and morphology from those in $Klf17^{+/+}$ mice (Fig. 6 *E* and *F*). Histological analysis indicated tissue necrosis in the abnormal embryos from $Klf17^{-/-}$ mice (*SI Appendix*, Fig. S8). Among 128 embryos from $Klf17^{+/+}$ mice that were examined, only 3 (3/128, 2.3%) appeared abnormal.

To determine if the fetal demise was caused by *Klf17* deficiency in male or female mice, we mated $Klf17^{+/+}$ and $Klf17^{-/-}$ mice with mice of the same or different genotype. Pups per litter from $Klf17^{-/-}$ females, whether mated with $Klf17^{+/+}$ or $Klf17^{-/-}$ males, were much fewer than those from $Klf17^{+/+}$ females, whether mated with $Klf17^{+/+}$ or $Klf17^{-/-}$ males (Fig. 6*G*). These results show that the fetal demise was due to Klf17 deficiency in female mice, regardless of the genotype in mating males or resulting fetuses, indicating the importance of Klf17 in the pregnant uterus but not in the placenta or other fetal tissues.

Trophoblast Invasion and Uterine Spiral Arteries in $Klf17^{-/-}$ Mice. Corin promotes trophoblast invasion and spiral artery remodeling in the pregnant uterus (15). We did histological and immunohistochemical analysis in pregnant $Klf17^{+/+}$ and $Klf17^{-/-}$ mice. At G12.5 d, we detected trophoblast invasion, as indicated by cytokeratin staining, in the decidua of $Klf17^{+/+}$ mice (Fig. 7 *A* and *B*). In comparison, trophoblast invasion was markedly reduced in the decidua of $Klf17^{-/-}$ mice (Fig. 7 *A* and *B*). At G18.5 d, decidual arteries in $Klf17^{+/+}$ mice were larger in diameter compared to those in $Klf17^{-/-}$ mice (Fig. 7 *C* and *D*). Unlike in $Klf17^{+/+}$ mice, the decidual arteries in $Klf17^{-/-}$ mice had more smooth muscle cells, as indicated by α-smooth muscle actin (SMA) staining (Fig. 7*D*). These results indicate that trophoblast invasion and uterine spiral artery remodeling are impaired in pregnant $Klf17^{-/-}$ mice.

Pregnancy-Induced Hypertension and Proteinuria in $Klf17^{-/-}$ Mice. Impaired trophoblast invasion and spiral artery remodeling contribute to preeclampsia, a disease characterized by gestational hypertension and proteinuria. We measured blood pressure in nonpregnant and pregnant $Klf17^{+/+}$ and $Klf17^{-/-}$ mice. Before pregnancy or at G12.5 d, $Klf17^{+/+}$ and $Klf17^{-/-}$ mice had similar blood pressures (Fig. 8*A*). At G18.5 d, blood pressures in $Klf17^{-/-}$ mice increased, compared to those in nonpregnancy or at G12.5 d (121.2 ± 1.3 [$n = 12$] vs. 104.6 ± 1.5 [$n = 14$] or 106.1 ± 2.3 [$n = 14$] mmHg; *P* values <0.001) or compared to those in $Klf17^{+/+}$ mice at G18.5 d (121.2 ± 1.3 [$n = 12$] vs. 103.6 ± 2.8 [$n = 8$] mmHg; $P < 0.001$) (Fig. 8*A*). These results indicate that $Klf17^{-/-}$ mice develop pregnancy-induced hypertension.

We next measured urinary protein levels in $Klf17^{+/+}$ and $Klf17^{-/-}$ mice. Similar urinary protein levels were found in $Klf17^{+/+}$ and $Klf17^{-/-}$ mice before pregnancy or at G12.5 d (Fig. 8*B*). At G18.5 d, urinary protein levels increased in $Klf17^{-/-}$, but not $Klf17^{+/+}$, mice (237.2 ± 12.9 [$n = 12$] vs. 103.4 ± 21.2 [$n = 7$] mg/dL; $P < 0.001$) (Fig. 8*B*). At postpartum day 7, blood pressure and urinary protein levels in $Klf17^{-/-}$ mice decreased to similar levels in control $Klf17^{+/+}$ mice (*SI Appendix*, Fig. S9).

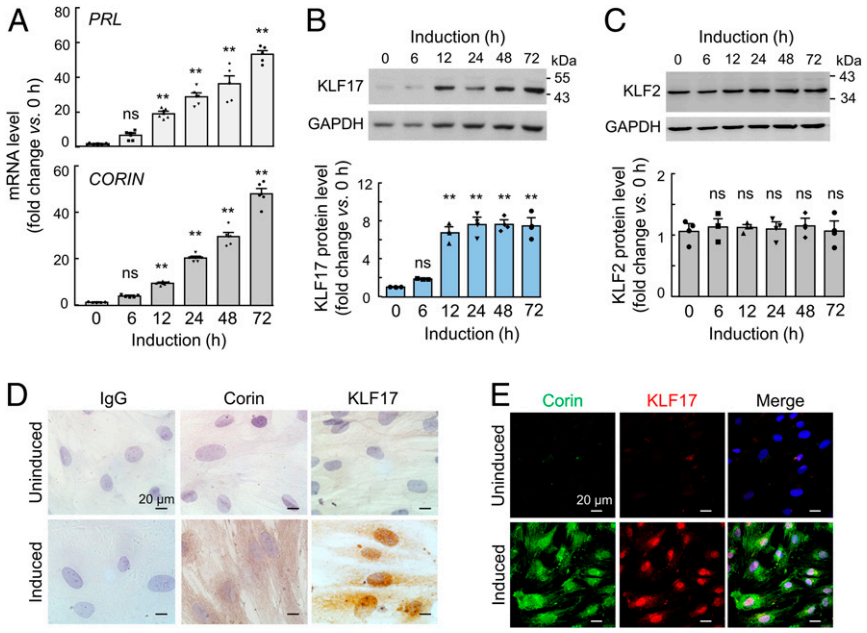

Fig. 4. KLF17 and KLF2 expression in decidualized HESCs. (*A*) Cultured HESCs were induced to undergo decidualization. *PRL* (*Top*) and *CORIN* (*Bottom*) mRNA levels at indicated time points were analyzed by qRT-PCR. (*B* and *C*) Western blotting of endogenous KLF17 (*B*) and KLF2 (*C*) proteins in HESCs cultured with the decidualization medium over time. GAPDH was used in Western blotting (*Top*) to calculate relative protein expression levels (*Bottom*). $n = 5$ per group in *A*; $n = 3$ per group in *B* and *C*. In bar graphs, data are presented as mean ± SEM; ns, not significant; $^{**}P < 0.01$ vs. the control at time 0 in the same experiment, as analyzed by ANOVA. (*D* and *E*) Immunohistochemistry (*D*) and coimmunofluorescent staining (*E*) of endogenous corin and KLF17 proteins in control (uninduced) and decidualized (induced) HESCs. In *D*, normal IgG was used as a negative control. Data are representative of three independent experiments. (Scale bars, 20 μm.)

In histological analysis, glomerular morphology in nonpregnant and pregnant *Klf17*$^{+/+}$ mice and nonpregnant *Klf17*$^{-/-}$ mice appeared normal in periodic acid–Schiff (PAS)-stained and Masson's trichrome-stained kidney sections (Fig. 8*C*). In pregnant *Klf17*$^{-/-}$ mice, especially at the late gestational stage (G18.5), ischemic glomeruli were observed, as indicated by capillaries of smaller diameters and fewer red blood cells (Fig. 8 *C* and *D*). These data indicate that *Klf17*$^{-/-}$ mice develop gestational kidney ischemia.

Discussion

In this study, we examined the mechanism underlying corin expression in the pregnant uterus. We identified KLF17 as a key transcription factor for uterine corin expression in pregnancy. This conclusion is supported by multiple lines of experimental evidence from *CORIN* promoter and ChIP analyses, uterine Klf protein profiling in ovariectomized mice treated with progesterone and normal pregnant mice, *KLF17* gene disruption in HESCs, and characterization of pregnant *Klf17*$^{-/-}$ mice. Our results reveal a KLF17-dependent transcriptional mechanism in uterine corin expression, which differs from the GATA-4–mediated mechanism in cardiac corin expression (23). Proteases, representing ∼2% of the proteins encoded by the human genome (30), are of great biological importance. Corin is a trypsin-like serine protease that has been shown to have such distinct transcriptional mechanisms in specific tissues.

KLF17 is a member of the KLF family, a group of structurally related transcription factors that act in diverse tissues to regulate a variety of physiological and pathological processes (27, 31, 32). Like all KLFs, KLF17 contains three conserved C-terminal DNA-binding zinc fingers which recognize GC-box and CACCC-box sequences (29, 33). Compared to other KLFs, mammalian KLF17 is far less known regarding its physiological function. Most studies of KLF17 focus on its role in tumor biology (34, 35). *KLF17* down-regulation has been identified in many human cancers, including breast, lung, liver, and stomach cancers (34, 36–38). It has been shown that KLF17 suppresses epithelial-mesenchymal transition and cancer metastasis in transforming growth factor β- and p53-mediated signaling mechanisms (34, 39, 40).

In zebrafish and *Xenopus*, the *klf17* gene is expressed in the blastula, lateral line neuromasts, and hatching glands (41–43). In chicken, embryonic *klf17* expression was detected in the primitive streak (44). Disruption of the *klf17* gene in zebrafish prevents the embryos from hatching, resulting in lethality (45). Similar results were found in *Xenopus* embryos when *klf17*, also called *Nepture*, was blocked by antisense oligonucleotides (46). These data demonstrate the importance of *klf17* in embryogenesis in early vertebrate species. Unlike fish and *Xenopus*, mammals do not have the hatching glands. In mice, high levels of *Klf17* (also called *Zfp393*) mRNA were found in spermatids and developing oocytes (29). *KLF17* mRNA expression also was reported in human testes (33), suggesting a potential role of mammalian KLF17 in gametogenesis. In our study, however, we found that both male and female *Klf17*$^{-/-}$ mice produced viable offspring, indicating that Klf17 is unnecessary for spermatogenesis and oocytogenesis in mice. Moreover, *Klf17*$^{-/-}$ and *Klf17*$^{+/+}$ mice had similar numbers of embryos at G12.5, indicating that ovulation, fertilization, and embryo implantation are not impaired by *Klf17* deficiency. We also observed the expected Mendelian ratio among offspring from *Klf17*$^{+/-}$ mating, indicating that Klf17 is dispensable in embryogenesis.

KLF members, including KLF5, KLF9, KLF11, and KLF13, have been implicated in uterine pathophysiology (47–52). In humans, KLF17 overexpression was reported in advanced endometrial cancers (53). In this study, we discovered an unexpected role of KLF17 in the pregnant uterus. We found that, upon progesterone stimulation, KLF17 expression was up-regulated in human uterine endometrial cells and the mouse pregnant uterus, which was associated with increased corin expression. Consistently, pregnant *Klf17*$^{-/-}$ mice lacked uterine corin expression. The mice

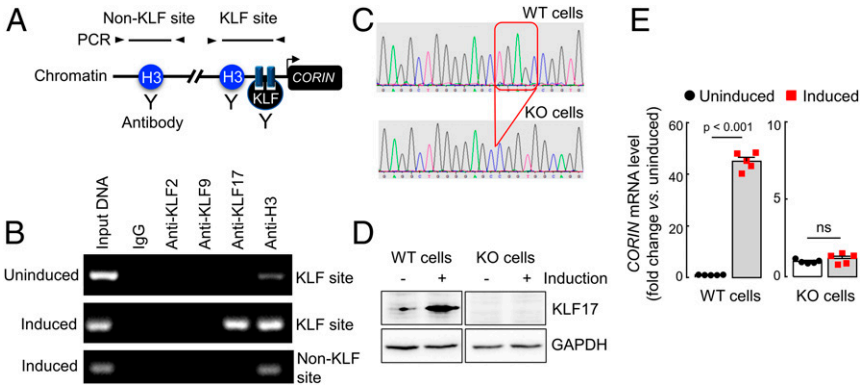

Fig. 5. ChIP analysis in HESCs and *CORIN* expression in *KLF17*-KO HESCs. (*A*) Illustration of ChIP assay in which chromatin fragments from uninduced and induced HESCs were precipitated with antibodies against histone 3 (H3) (positive control) or KLF proteins and used for PCR with primers for non-KLF and KLF sites. (*B*) PCR products are shown in agarose gels. (*C*) The *KLF17* gene was disrupted in HESCs using CRISPR/Cas9. Partial sequencing data from WT and *KLF17*-KO HESCs are shown. Red box indicates the deleted sequence. (*D*) Western blotting of endogenous KLF17 protein in WT and *KLF17*-KO HESCs without (–) or with (+) decidualization (induction). GAPDH was a control. Nonadjacent lanes from the same Western blot are presented. Data are representative of three independent experiments. (*E*) Relative *CORIN* mRNA levels in WT and *KLF17*-KO HESCs without (uninduced) or with (induced) decidualization. $n = 5$ per group. Data are presented as mean ± SEM; *P* values were analyzed by two-tailed Student's *t* test. ns, not significant.

also had delayed trophoblast invasion, poorly remodeled uterine spiral arteries, and smaller litter sizes, a similar phenotype reported in corin- and ANP-deficient mice (15). Moreover, *Klf17*$^{-/-}$ mice developed late gestational hypertension and proteinuria, which was also observed in corin- and ANP-deficient mice (15). These results support a crucial role of KLF17 in corin expression and uterine biology. As a transcription factor, KLF17 is expected to regulate other genes in the pregnant uterus. Further studies are important to identify those KLF17-dependent genes and to understand their role in regulating uterine physiology in pregnancy.

In summary, uterine spiral artery remodeling is a physiological mechanism in pregnancy. Corin is a protease that promotes spiral artery remodeling in the pregnant uterus. Low levels of *CORIN* mRNA have been identified in patients with preeclampsia (15), suggesting a potential role of defective *CORIN* transcription in the disease. Here we show that KLF17 is necessary for *CORIN* up-regulation in human uterine endometrial cells and that *Klf17* deficiency abolishes uterine *Corin* expression in mice. Our results indicate that KLF17 is an important transcription factor that regulates corin expression and uterine biology in pregnancy.

Materials and Methods

Plasmids. The pGL3-based firefly luciferase plasmid (Promega) containing a 405-bp human *CORIN* promoter sequence and the pRL-SV40 plasmid expressing Renilla luciferase (Promega) were described previously (23).

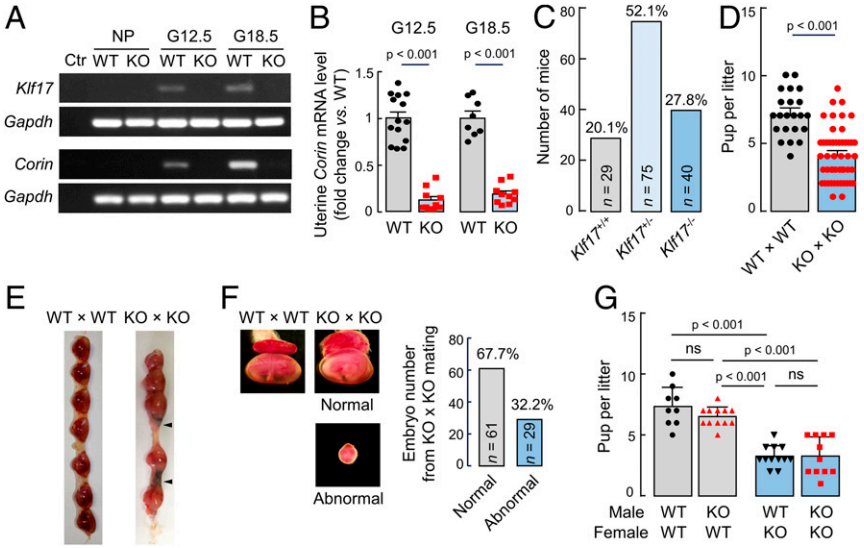

Fig. 6. Gene expression and fertility in *Klf17*$^{-/-}$ mice. (*A*) *Klf17* and *Corin* mRNA levels in uteruses from nonpregnant (NP) and pregnant (G12.5 and G18.5) WT and *Klf17*$^{-/-}$ (KO) mice, as analyzed by RT-PCR. Samples, in which cDNA templates were omitted, were negative controls (Ctr). (*B*) Relative *Corin* mRNA levels in pregnant (G12.5 and G18.5) WT and KO mice, as analyzed by qRT-PCR. $n = 8$ to 14 per group. (*C*) Number and percentage of *Klf17*$^{+/+}$, *Klf17*$^{+/-}$, and *Klf17*$^{-/-}$ pups in 28 litters from 18 *Klf17*$^{+/-}$ mice. (*D*) Number of pups per litter from WT × WT ($n = 22$) and KO × KO ($n = 52$) mating. (*E*) Representative images of embryos from G12.5 WT and KO females mated with males of the same genotype. Arrowheads indicate abnormal embryos. (*F*) Representative images of higher magnification (×16) showing a normal embryo from a WT mouse and two embryos (one normal and one abnormal) from a KO mouse. The bar graph shows percentages of normal and abnormal embryos in a total of 90 embryos from KO mice. (*G*) Number of pups per litter from WT and KO females mated with WT or KO males. Data are presented as mean ± SEM; *P* values were analyzed by two-tailed Student's *t* test (*B* and *D*) or ANOVA (*G*). ns, not significant.

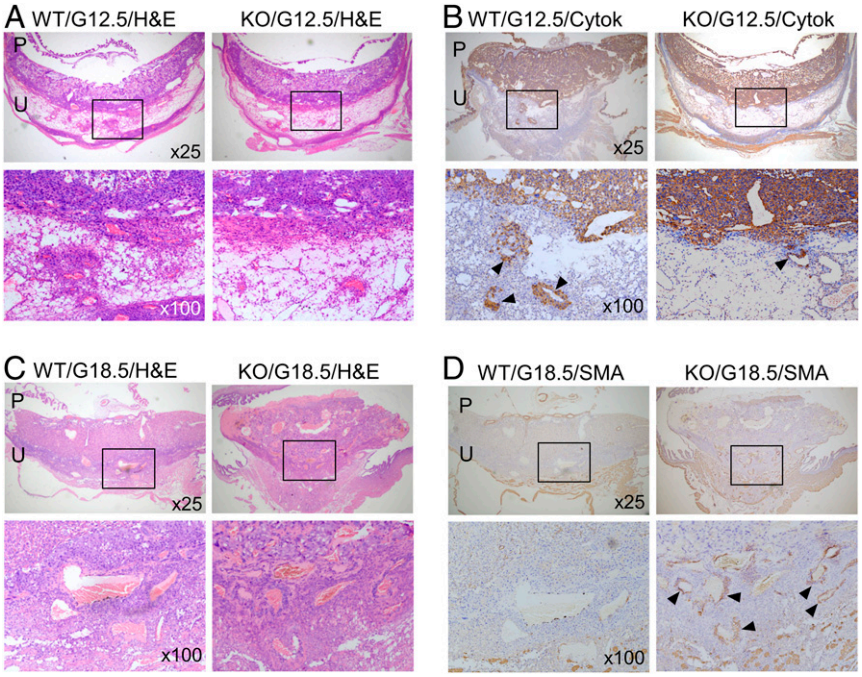

Fig. 7. Trophoblast invasion and spiral artery remodeling in *Klf17*$^{-/-}$ mice. (*A* and *B*) Placental (P) and uterine (U) sections from WT and *Klf17*$^{-/-}$ (KO) mice at G12.5 were stained with H&E (*A*) or immune-stained with an anti-cytokeratin 18 (Cytok) antibody (*B*). Boxed areas in low-magnification (×25) images (*Top* row) are shown at a higher magnification (×100) (*Bottom* row). Endovascular trophoblast invasion in decidual sections are indicated by arrowheads. (*C* and *D*) Placental (P) and uterine (U) sections from WT and KO mice at G18.5 were stained with H&E (*C*) or immune-stained with an anti-SMA antibody (*D*). Boxed areas of low-magnification (×25) images (*Top* row) are shown at a higher magnification (×100) (*Bottom* row). Positive SMA staining in decidual arteries in KO mice are indicated by arrowheads. Data are representative of studies in at least five mice per group.

Additional plasmids with serial deletions in the *CORIN* promoter sequence were made by site-directed mutagenesis (Agilent Technologies). Plasmids expressing human KLF2 (RC210042), KLF9 (RC210147), KLF15 (RC207523), and KLF17 (RC208293) proteins were from OriGene. The KLF proteins expressed by the pCMV6-based plasmids contained a C-terminal Myc-DDK (FLAG) tag for protein detection.

Cell Culture. Murine HL-1 cardiomyocytes, originally from William Claycomb, Louisiana State University Medical Center, New Orleans, LA (no mycoplasma contamination), were cultured in Claycomb medium (Sigma) with 10% fetal bovine serum (FBS) and 4 mM L-glutamine. Human uterine endometrial adenocarcinoma AN3-CA cells (ATCC HTB-111; short tandem repeat (STR) profiled; no mycoplasma contamination) and HESCs (ATCC CRL-4003; STR profiled; no mycoplasma contamination) were cultured, respectively, in minimum Eagle's medium (MEM) (HyClone, SH30024.01B) with 10% FBS and Dulbecco's Modified Eagle Media (DMEM)/Ham's F-12 medium (Sigma) with 10% charcoal-dextran stripped FBS (Biological Industries), 1.5 g/L sodium bicarbonate, and 1% insulin, transferrin, and selenium (Sigma). The cells were cultured at 37 °C in humidified incubators with 5% CO_2.

Dual-Luciferase Reporter Assay. The luciferase plasmids with human *CORIN* promoter fragments and the control pGL3 plasmid were transfected into AN3-CA and HL-1 cells with Lipofectamine 2000 reagent (Thermo Fisher). The pRL-SV40 plasmid expressing *Renilla* luciferase was cotransfected as a control for transfection efficiency. After 40 h at 37 °C, the transfected cells were lysed with the buffer provided in the Dual-Luciferase Reporter Assay kit (Promega). After 15 min at room temperature, a luciferase assay buffer was added, and firefly and *Renilla* luciferase activities were measured, sequentially, in Luminoskan Ascent microplate reader (Thermo Fisher). *CORIN* promoter activities were calculated based on the normalized firefly luciferase activity.

Western Blotting of Recombinant KLFs in Transfected Cells. To examine the effect of KLF expression on *CORIN* promoter activity, plasmids expressing human KLF2, KLF9, KLF15, and KLF17 were transfected into AN3-CA and HL-1 cells with Lipofectamine 2000 (Thermo Fisher). After 40 h at 37 °C, the cells were lysed with 25 mM Tris·HCl, pH 7.4, 150 mM NaCl, 1 mM ethylenediaminetetraacetic acid, 1% (vol/vol) Nonidet P-40, 5% (vol/vol) glycerol, and 2% (vol/vol) protease inhibitor mixture (Thermo Fisher, 78442). Proteins were mixed with a sample buffer with 2% β-mercaptoethanol and analyzed by sodium dodecyl sulfate/polyacrylamide gel electrophoresis and Western blotting using antibodies against FLAG (Sigma, A8592, 1:5,000) and glyceraldehyde 3-phosphate dehydrogenase (GAPDH) (Multi Science Biotech, ab011-04, 0.125 μg/mL).

HESCs. HESCs were induced to undergo decidualization in DMEM/F12 medium with 1 μM medroxyprogesterone acetate (Sigma), 10 nM estradiol (Cayman Chemical), and 0.5 mM 8-bromo-cAMP (Sigma). The cells with the regular DMEM/F12 medium were used as controls. At different time points, the cells were lysed, as described above. qRT-PCR (described below) was done to analyze *PRL*, encoding prolactin (decidualization marker), and *CORIN* mRNA levels. Western blotting was used to analyze endogenous KLF proteins using antibodies against KLF2 (Abcam, ab203591, 1 μg/mL) and KLF17 (Abcam, ab84196, 2 μg/mL). Relative protein levels on Western blot-derived X-ray films were quantified by densitometry. For immunohistochemistry, HESCs on coverslips were fixed with 10% paraformaldehyde and immunostained with antibodies against Corin (made in the laboratory) (15), KLF2 (Abcam, ab203591, 5 μg/mL), and KLF17 (Abcam, ab84196, 5 μg/mL) or normal IgG (Bioworld Technology, BD0051, 2 μg/mL), followed with a horseradish peroxidase (HRP)-conjugated secondary antibody (supplied with a GTVision kit, Gene Tech, GK5007). After incubation at 4 °C overnight followed by washing, an HRP substrate (3, 3′-diaminobenzidine) solution was added, and the cells were examined under a microscope (Olympus, DP73). For immunofluorescent staining, secondary antibodies conjugated with Alexa-488 (green) or 594 (red) (Invitrogen, A21202 and A11012) were used. Cell nuclei were stained with DAPI (SouthernBiotech) before confocal microscopy (Olympus, FV1000).

RT-PCR and qRT-PCR. Total RNAs were isolated from cultured cells or mouse tissues using TRIzol reagent (Invitrogen) or RNeasy kit (Qiagen) or High Pure RNA Isolation kit (Omega Bio-tek) to make first-strand complementary DNAs (cDNAs) with High Capacity cDNA Reverse Transcription kit (Thermo Fisher). RT-PCR and qRT-PCR were done with oligonucleotide primers (*SI Appendix*, Table S1) for mouse *Corin* and *Klf*s or human *CORIN* and *PRL* genes. For qRT-PCR, the reaction was done in a 20-μL mixture with 10 μL of LightCycler SYBR Green Master Mix (Roche, 04707516001), cDNA templates (17.5 ng), and oligonucleotide primers (10 pM each) in 40 cycles. The results were analyzed

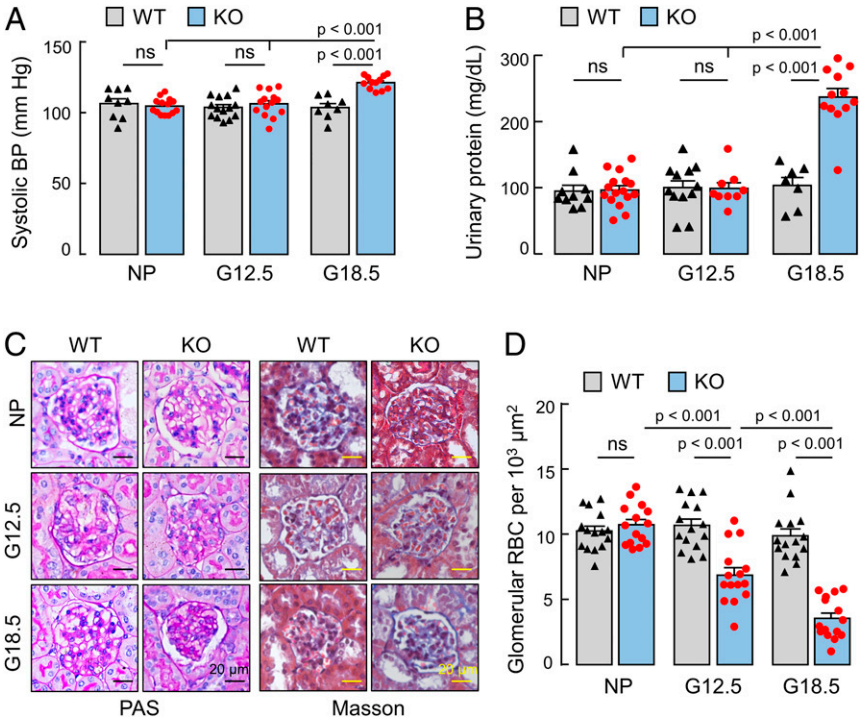

Fig. 8. Hypertension, proteinuria, and ischemic glomeruli in *Klf17*$^{-/-}$ mice. (*A*) Systolic blood pressure (BP) in nonpregnant (NP) and pregnant (G12.5 and G18.5) WT and *Klf17*$^{-/-}$ (KO) mice. $n = 8$ to 14 per group. (*B*) Urinary protein levels in NP and pregnant (G12.5 and G18.5) WT and KO mice. $n = 7$ to 16 per group. (*C*) Glomerular histology in PAS-stained and Masson's trichrome-stained renal sections from NP and pregnant (G12.5 and G18.5) WT and KO mice. (Scale bars, 20 μm). (*D*) Glomerular red blood cells (RBC) were counted in renal sections from NP and pregnant (G12.5 and G18.5) WT and KO mice. In *A*, *B*, and *D*, data are presented as mean ± SEM; *P* values were analyzed by ANOVA; ns, not significant.

using LightCycler 480 software (Roche). Relative mRNA levels were calculated with values of *GAPDH* or *Gapdh* gene as references.

ChIP. ChIP was done using the SimpleChIP Plus Enzymatic Chromatin IP kit (Cell Signaling Technology). Uninduced and induced HESCs were treated with 1% formaldehyde for 10 min at room temperature and lysed in a buffer containing dithiothreitol and protease inhibitors. The lysates were treated with micrococcal nuclease to generate chromatin fragments for immunoprecipitation with magnetic beads and antibodies against KLF2 (Abcam, ab203591, 1 μg), KLF9 (Abcam, ab26076, 1 μg), KLF17 (Abcam, ab84196, 1 μg), and Histone 3 (H3) (supplied with the ChIP kit, 10 μL) (positive control) or normal IgG (Bioworld Technology, BD0051, 1 μg) (negative control). The bound chromatins were eluted from the beads. DNAs were separated by heating, purified with a spin column, and used for PCR and qPCR with primers for the KLF site in the *CORIN* promoter (5′-GGA GGA TCT GTC ATT ACG GGT T-3′ and 5′-CAA GCT CAA GAG AGA CAA ACT GAA C-3′) or a non-KLF site (5′-CGG AGG ATC TGT CAT TAC GGG-3′ and 5′-CTG CTC TAC AGA TCC CAC CC-3′).

***KLF17* Knockout in HESCs with CRISPR/Cas9.** Three pairs of small guide RNAs (sgRNAs) targeting the *KLF17* gene (exon 1) were designed with online tools at a CRISPR/Cas9 website (https://wge.stemcell.sanger.ac.uk//find_crisprs). The primers—guide RNA (gRNA)-K*LF17*-1F (5′-CAC CGG CTG AGA TGG AAC AGG AGG CT-3′), gRNA-*KLF17*-1R (5′-AAA CAG CCT CCT GTT CCA TCT CAG CC-3′), gRNA-*KLF17*-2F (5′-CAC CGG GTC CCC TTT GGT GTC TGT TG -3′), gRNA-*KLF17*-2R (5′-AAA CCA ACA GAC ACC AAA GGG GAC CC-3′), gRNA-*KLF17*-3F (5′-CAC CGG AGA GAT GCT GGG GTC CCC TT-3′), and gRNA-*KLF17*-3R (5′-AAA CAA GGG GAC CCC AGC ATC TCT CC-3′)—were annealed and cloned into PX458 plasmid (Addgene) expressing Cas9-sgRNA for transfection in HESCs. The cells expressing green fluorescent protein (an indicator) selected by flow cytometry were grown in individual colonies after limiting dilution and verification by PCR, followed by DNA sequencing, and Western blotting for *KLF17* knockout.

Mouse Studies. Experiments involving mice were approved by the Animal Care and Use Committee at Soochow University and conducted in accordance with the guidelines for the ethical treatment and handling of animals in research. Mice were housed in temperature-controlled rooms with 12-h/12-h light-dark cycles and fed with a standard rodent chow diet and ad libitum access to water. The sample size was based on pilot and published comparable studies. The investigators who performed the experiments were not blinded to mouse genotypes.

Ovariectomy was performed in anesthetized C57BL/6 females (8 to 10 wk old). After 9 d of recovery, the mice were randomly divided into three groups to receive subcutaneous injection of sesame oil (vehicle) (100 μL), estradiol (Cayman Chemical) (50 ng in 100 μL sesame oil), or progesterone (Sigma) (1 mg in 100 μL sesame oil), respectively. After 3 d of daily injection, the mice were euthanized and uterus tissues were isolated for gene expression analysis. In parallel, C57BL/6 females (8 to 10 wk old) were mated with C57BL/6 males (8 to 10 wk old) and checked for vaginal plugs. The day on which a vaginal plug was observed was defined as G0.5 d. At different G days, uteruses and embryos were isolated for gene, protein, and tissue analyses.

Generation of *Klf17*$^{-/-}$ Mice. Mouse embryonic stem cells (clone ID: EPD0099_1_D12) were generated at the Wellcome Trust Sanger Institute to have a disrupted *Klf17* allele (*Klf17*$^{tm1a(KOMP)Wtsi}$) with a neo cassette and loxP sites flanking exon 2. The cells were used for blastocyst injection to make chimeric and subsequent *Klf17*$^{+/tm1a}$ mice in a C57BL/6 background. Genotyping was done by PCR with primers *Klf17*-F (5′-GGT TTC TTT CTG TAA TCC TGG CTA T-3′) and *Klf17*-KO-R (5′-CAC AAC GGG TTC TTC TGT TAG TC-3′) or *Klf17*-WT-R (5′-TGC CAT AAC ACT GGT AAA CAA CC-3′). *Klf17*$^{+/tm1a}$ mice were bred to produce *Klf17*$^{+/+}$, *Klf17*$^{+/tm1a}$, and *Klf17*$^{tm1a/tm1a}$ littermates for further analyses. *Klf17*$^{+/tm1a}$ and *Klf17*$^{tm1a/tm1a}$ mice are referred to as *Klf17*$^{+/-}$ and *Klf17*$^{-/-}$ mice, respectively, in this study.

Blood Pressure Measurement. Blood pressure in mice was measured using a computerized noninvasive photoelectric tail-cuff system (BP-2000, Visitech Systems). Mice were placed on a prewarmed specimen platform under a cover with their tails in the cuff, allowing them to acclimate to the apparatus and the room environment. Each practice run lasted no more than 30 min. After 3 d of acclimation, which was done at the same time of the day and by the same handlers, systolic blood pressure was measured. Each measurement

included 5 preconditioning cycles and 20 regular cycles with 5 s between two cycles and maximal cuff pressure of 150 mmHg. The mean values of blood pressure were recorded.

Urinary Proteins. Urine samples were collected from nonpregnant and pregnant (G12.5 and G18.5) mice. Urinary protein levels were measured using a Bradford colorimetric assay (Nanjing Jiancheng Bioengineering Institute, C035-2) and bovine serum albumin as a reference standard.

Tissue Histology, Immunohistochemistry, and Western Blotting. Mouse tissues were fixed with 4% (vol/vol) formalin and embedded in paraffin. Sections (5 μm in thickness) were cut and mounted on gelatin-coated slides. Serial sections were used for staining with hematoxylin and eosin (H&E), PAS, and Masson's trichrome or immunohistochemistry based on published methods (8, 15). Antibodies against cytokeratin 18 (Abcam, ab181597, 1.25 μg/mL) and SMA (Abcam, ab5694, 1 μg/mL) or a normal IgG (Bioworld Technology, BD0051) (negative control) were used. An HRP-conjugated secondary antibody (supplied with the MaxVision kit, kit-5005, Maxim Biotechnologies) was used for detection. Stained sections were examined under a microscope (Leica DM2000 LED). For Western blotting, uterus and control heart and liver samples were homogenized in a lysis solution (25). Protein levels were quantified using a bicinchoninic acid assay (Thermo Scientific, 23227). Western blotting was done with primary antibodies against Klf17 (Abcam, ab84196, 1:500) and corin (15) (1:1,000) and an HRP-conjugated secondary antibody (Bioworld Technology, bs13278, 1:10000). In these experiments, recombinant KLF17 and corin expressed in HEK293 cells were used as positive controls. GAPDH was used as a loading control.

For immunohistochemical analysis of trophoblast invasion, tissues from at least five mice per group and at least two implantation sites per mouse were used. Serial sections (>40 per embryo) were prepared. The position of the maternal artery was used as a guide to orient section positions. Cytokeratin 18-stained slides were examined independently by two individuals. The sections with the deepest trophoblast invasion are presented in Fig. 7. For glomerular histology, renal sections were stained with PAS and Masson's trichrome. In Masson's trichrome-stained sections, red blood cells in glomeruli were counted under a microscope by two individuals in a blinded manner. Each study group included at least three mice. The data were from at least five randomly selected fields in at least three sections from each mouse.

Statistical Analysis. The analysis was done using Prism 7 (Graphpad). Differences were analyzed by two-tailed Student's *t* test to compare two groups or ANOVA followed by Tukey's post hoc analysis to compare three or more groups. *P* values of <0.05 were considered to be statistically significant. Data are presented as mean ± SD or SEM, as indicated.

Data Availability Statement. All data described in the paper are presented in the main text or *SI Appendix*.

ACKNOWLEDGMENTS. We thank Junliang Pan for helping with gene promoter analysis. This work was supported in part by grants from the National Natural Science Foundation of China (81873840, 81671485, 81570457, and 31500636), the National Basic Research Program of China (2015CB943302), and the Priority Academic Program Development of Jiangsu Higher Education Institutes. Mouse production was supported by a grant from the Ministry of Science and Technology of China (2018YFA0801100).

1. R. Pijnenborg, L. Vercruysse, M. Hanssens, The uterine spiral arteries in human pregnancy: Facts and controversies. *Placenta* **27**, 939–958 (2006).
2. T. Chaiworapongsa, P. Chaemsaithong, L. Yeo, R. Romero, Pre-eclampsia part 1: Current understanding of its pathophysiology. *Nat. Rev. Nephrol.* **10**, 466–480 (2014).
3. S. J. Fisher, Why is placentation abnormal in preeclampsia? *Am. J. Obstet. Gynecol.* **213** (suppl.), S115–S122 (2015).
4. C. W. Redman, I. L. Sargent, Latest advances in understanding preeclampsia. *Science* **308**, 1592–1594 (2005).
5. W. Song, H. Wang, Q. Wu, Atrial natriuretic peptide in cardiovascular biology and disease (NPPA). *Gene* **569**, 1–6 (2015).
6. W. Yan, F. Wu, J. Morser, Q. Wu, Corin, a transmembrane cardiac serine protease, acts as a pro-atrial natriuretic peptide-converting enzyme. *Proc. Natl. Acad. Sci. U.S.A.* **97**, 8525–8529 (2000).
7. Y. Zhou, Q. Wu, Corin in natriuretic peptide processing and hypertension. *Curr. Hypertens. Rep.* **16**, 415 (2014).
8. L. Dong *et al*., Localization of corin and atrial natriuretic peptide expression in human renal segments. *Clin. Sci. (Lond.)* **130**, 1655–1664 (2016).
9. T. Ichiki *et al*., Corin is present in the normal human heart, kidney, and blood, with pro-B-type natriuretic peptide processing in the circulation. *Clin. Chem.* **57**, 40–47 (2011).
10. F. Theilig, Q. Wu, ANP-induced signaling cascade and its implications in renal pathophysiology. *Am. J. Physiol. Renal Physiol.* **308**, F1047–F1055 (2015).
11. D. Enshell-Seijffers, C. Lindon, B. A. Morgan, The serine protease Corin is a novel modifier of the Agouti pathway. *Development* **135**, 217–225 (2008).
12. S. J. Luo, Y. C. Liu, X. Xu, Tigers of the world: Genomics and conservation. *Annu. Rev. Anim. Biosci.* **7**, 521–548 (2019).
13. R. C. Nordberg, H. Wang, Q. Wu, E. G. Loboa, Corin is a key regulator of endochondral ossification and bone development via modulation of vascular endothelial growth factor A expression. *J. Tissue Eng. Regen. Med.* **12**, 2277–2286 (2018).
14. H. Zhou, J. Zhu, M. Liu, Q. Wu, N. Dong, Role of the protease corin in chondrogenic differentiation of human bone marrow-derived mesenchymal stem cells. *J. Tissue Eng. Regen. Med.* **12**, 973–982 (2018).
15. Y. Cui *et al*., Role of corin in trophoblast invasion and uterine spiral artery remodelling in pregnancy. *Nature* **484**, 246–250 (2012).
16. T. J. Kaitu'u-Lino *et al*., Corin, an enzyme with a putative role in spiral artery remodeling, is up-regulated in late secretory endometrium and first trimester decidua. *Hum. Reprod.* **28**, 1172–1180 (2013).
17. D. W. Armstrong *et al*., Gestational hypertension in atrial natriuretic peptide knockout mice and the developmental origins of salt-sensitivity and cardiac hypertrophy. *Regul. Pept.* **186**, 108–115 (2013).
18. D. W. Armstrong *et al*., Gestational hypertension and the developmental origins of cardiac hypertrophy and diastolic dysfunction. *Mol. Cell. Biochem.* **391**, 201–209 (2014).
19. N. Dong *et al*., Corin mutations K317E and S472G from preeclamptic patients alter zymogen activation and cell surface targeting. *J. Biol. Chem.* **289**, 17909–17916 (2014). Correction in: J. Biol. Chem. 289, 21298 (2014).
20. A. Stepanian *et al*.; ECLAXIR Study Group, Highly significant association between two common single nucleotide polymorphisms in CORIN gene and preeclampsia in Caucasian women. *PLoS One* **9**, e113176 (2014).
21. D. Durocher, M. Nemer, Combinatorial interactions regulating cardiac transcription. *Dev. Genet.* **22**, 250–262 (1998).
22. J. D. Molkentin *et al*., A calcineurin-dependent transcriptional pathway for cardiac hypertrophy. *Cell* **93**, 215–228 (1998).
23. J. Pan *et al*., Genomic structures of the human and murine corin genes and functional GATA elements in their promoters. *J. Biol. Chem.* **277**, 38390–38398 (2002).
24. R. J. Arceci, A. A. King, M. C. Simon, S. H. Orkin, D. B. Wilson, Mouse GATA-4: A retinoic acid-inducible GATA-binding transcription factor expressed in endodermally derived tissues and heart. *Mol. Cell. Biol.* **13**, 2235–2246 (1993).
25. S. Chen *et al*., PCSK6-mediated corin activation is essential for normal blood pressure. *Nat. Med.* **21**, 1048–1053 (2015).
26. W. Yan, N. Sheng, M. Seto, J. Morser, Q. Wu, Corin, a mosaic transmembrane serine protease encoded by a novel cDNA from human heart. *J. Biol. Chem.* **274**, 14926–14935 (1999).
27. B. B. McConnell, V. W. Yang, Mammalian Krüppel-like factors in health and diseases. *Physiol. Rev.* **90**, 1337–1381 (2010).
28. H. Zhu, C. C. Hou, L. F. Luo, Y. J. Hu, W. X. Yang, Endometrial stromal cells and decidualized stromal cells: Origins, transformation and functions. *Gene* **551**, 1–14 (2014).
29. W. Yan, K. H. Burns, L. Ma, M. M. Matzuk, Identification of Zfp393, a germ cell-specific gene encoding a novel zinc finger protein. *Mech. Dev.* **118**, 233–239 (2002).
30. C. M. Overall, C. P. Blobel, In search of partners: Linking extracellular proteases to substrates. *Nat. Rev. Mol. Cell Biol.* **8**, 245–257 (2007).
31. Y. Fan *et al*., Krüppel-like factors and vascular wall homeostasis. *J. Mol. Cell Biol.* **9**, 352–363 (2017).
32. P. N. Hsieh, L. Fan, D. R. Sweet, M. K. Jain, The Krüppel-like factors and control of energy homeostasis. *Endocr. Rev.* **40**, 137–152 (2019).
33. J. van Vliet *et al*., Human KLF17 is a new member of the Sp/KLF family of transcription factors. *Genomics* **87**, 474–482 (2006).
34. K. Gumireddy *et al*., KLF17 is a negative regulator of epithelial-mesenchymal transition and metastasis in breast cancer. *Nat. Cell Biol.* **11**, 1297–1304 (2009).
35. S. Zhou, X. Tang, F. Tang, Krüppel-like factor 17, a novel tumor suppressor: Its low expression is involved in cancer metastasis. *Tumour Biol.* **37**, 1505–1513 (2016).
36. X. D. Cai *et al*., Reduced expression of Krüppel-like factor 17 is related to tumor growth and poor prognosis in lung adenocarcinoma. *Biochem. Biophys. Res. Commun.* **418**, 67–73 (2012).
37. F. Y. Liu *et al*., Down-regulated KLF17 expression is associated with tumor invasion and poor prognosis in hepatocellular carcinoma. *Med. Oncol.* **30**, 425 (2013).
38. J. J. Peng *et al*., Reduced Krüppel-like factor 17 (KLF17) expression correlates with poor survival in patients with gastric cancer. *Arch. Med. Res.* **45**, 394–399 (2014).
39. A. Ali *et al*., Tumor-suppressive p53 signaling empowers metastatic inhibitor KLF17-dependent transcription to overcome tumorigenesis in non-small cell lung cancer. *J. Biol. Chem.* **290**, 21336–21351 (2015).
40. A. Ali *et al*., KLF17 empowers TGF-β/Smad signaling by targeting Smad3-dependent pathway to suppress tumor growth and metastasis during cancer progression. *Cell Death Dis.* **6**, e1681 (2015).
41. T. L. Huber *et al*., Neptune, a Krüppel-like transcription factor that participates in primitive erythropoiesis in Xenopus. *Curr. Biol.* **11**, 1456–1461 (2001).
42. A. Kawahara, I. B. Dawid, Expression of the Krüppel-like zinc finger gene biklf during zebrafish development. *Mech. Dev.* **97**, 173–176 (2000).

43. K. Kotkamp, R. Mössner, A. Allen, D. Onichtchouk, W. Driever, A Pou5f1/Oct4 dependent Klf2a, Klf2b, and Klf17 regulatory sub-network contributes to EVL and ectoderm development during zebrafish embryogenesis. *Dev. Biol.* **385**, 433–447 (2014).
44. P. B. Antin, M. Pier, T. Sesepasara, T. A. Yatskievych, D. K. Darnell, Embryonic expression of the chicken Krüppel-like (KLF) transcription factor gene family. *Dev. Dyn.* **239**, 1879–1887 (2010).
45. H. Suzuki *et al*., Characterization of biklf/klf17-deficient zebrafish in posterior lateral line neuromast and hatching gland development. *Sci. Rep.* **9**, 13680 (2019).
46. T. Kurauchi, Y. Izutsu, M. Maéno, Involvement of Neptune in induction of the hatching gland and neural crest in the Xenopus embryo. *Differentiation* **79**, 251–259 (2010).
47. G. S. Daftary *et al*., A novel role of the Sp/KLF transcription factor KLF11 in arresting progression of endometriosis. *PLoS One* **8**, e60165 (2013).
48. M. E. Heard, C. D. Simmons, F. A. Simmen, R. C. Simmen, Krüppel-like factor 9 deficiency in uterine endometrial cells promotes ectopic lesion establishment associated with activated notch and hedgehog signaling in a mouse model of endometriosis. *Endocrinology* **155**, 1532–1546 (2014).
49. M. E. Heard, M. C. Velarde, L. C. Giudice, F. A. Simmen, R. C. Simmen, Krüppel-like factor 13 deficiency in uterine endometrial cells contributes to defective steroid hormone receptor signaling but not lesion establishment in a mouse model of endometriosis. *Biol. Reprod.* **92**, 140 (2015).
50. J. M. Pabona *et al*., Krüppel-like factor 9 and progesterone receptor coregulation of decidualizing endometrial stromal cells: Implications for the pathogenesis of endometriosis. *J. Clin. Endocrinol. Metab.* **97**, E376–E392 (2012).
51. R. C. Simmen *et al*., Subfertility, uterine hypoplasia, and partial progesterone resistance in mice lacking the Kruppel-like factor 9/basic transcription element-binding protein-1 (Bteb1) gene. *J. Biol. Chem.* **279**, 29286–29294 (2004).
52. X. Sun *et al*., Kruppel-like factor 5 (KLF5) is critical for conferring uterine receptivity to implantation. *Proc. Natl. Acad. Sci. U.S.A.* **109**, 1145–1150 (2012).
53. P. Dong *et al*., Identification of KLF17 as a novel epithelial to mesenchymal transition inducer via direct activation of TWIST1 in endometrioid endometrial cancer. *Carcinogenesis* **35**, 760–768 (2014).